International Journal of Applied Engineering Research ISSN 0973-4562 Volume 10, Number 18 (2015) pp 38693-38697

Numerical study on the heat dissipation of a vacuum compatible motor

Chan Byon[#], Juhee Lee[*]

*School of Mechanical Engineering, Yeungnam University, Gyeongsan, Gyeongbuk 38541, Republic of Korea These two authors equally contributed to this work. # cbyon@ynu.ac.kr * hyesung426@naver.com*

Dong-Yeon Lee

School of Mechanical Engineering, Yeungnam University, Gyeongsan, Gyeongbuk 38541, Republic of Korea Corresponding author dylee@ynu.ac.kr

Abstract

We developed a novel cylindrical magnetic levitation stage that provides rotational motion with high precision in a vacuum environment. The heat dissipation from a magnetic levitation stage is investigated numerically. In order to facilitate heat transfer from the inner space vacuum, a copper pipe is inserted in the coil base of the stator to circulate cooling water. The modules are analyzed using the finite element method (FEM) to determine the effects of the electrical current and the flow velocity of the cooling water. The results indicate that the augmentation of the cooling pipe brings about a significant enhancement in the heat dissipation performance of the magnetic levitation stage. The coil temperature is shown to decrease as the flow rate increases, or as the current decreases. The proposed cooling scheme sheds light on an optimal design for a vacuum-based electromagnetic system. This, in turn, could significantly affect next-generation semiconductor manufacturing.

Keywords: Stage design, heat transfer, magnetic levitation stage, numerical analysis.

Introduction

With the advent of nanotechnology, the use of high precision stages is rapidly increasing in the field of nanoscale patterning. The magnetic levitation stage is regarded as a promising option for a high precision positioning mechanism [1]. It has many advantages over a conventional mechanical stage in that it does not require a tight bearing tolerance, and does not need expensive piezoelectric systems [2]. In this regard, various types of magnetic levitation stages have been developed and analyzed [2-7]. Sawyer [3] first presented a magnetically levitated stage for focusing and alignment, and large planar motions for positioning, using a single magnetically levitated moving part, (a platen). Shan [4] proposed a motion control technique with ultra-high precision for a magnetic suspension stage. Chen [5] developed a dual-axis repulsive maglev guiding system that uses a permanent magnet. More recently, Kim [2] designed and implemented a novel planar magnetic levitator with four permanent magnet linear motors. This pioneering work was extended by Jeon [6], who developed a state-of-the-art magnetic levitation system that can handle six degree of freedom movement (x, y, z, θ_x, θ_y, θ_z) in both wafer size and nanoscale positioning. Jeon also developed a novel cylindrical magnetic levitation stage to overcome the shortcomings of the planar stage, and to efficiently provide levitation, rotational, and translational movement [7]. Due to its novelty and technological advantages, it is often called the third generation magnetic levitation stage [7]. The basic various heat transfer theories are explained in detail in the literature [8]. The optimization of various heat transfer mechanism is well explained [9]. Temperature rise of a permanent magnet linear motor has been calculated with consideration of the thermal conduction and heat convection mechanism in the air [10]. The vacuum condition, accordingly the radiative heat transfer was not considered. The transient heat conduction through a water jacket of a permanent magnet linear motor in the air is analyzed in ref. [11]. The heat transfer analysis of a linear motor driven stage was performed by using a simplified thermal resistance modeling and verified with a finite element analysis [12]. Temperature calcuation for tubular linear motor in ambient conditions has been performed[13]. A transient lumped-parameter thermal model of an induction motor has been proposed[14]. Various thermal analysis including computational fluid dynamics for the electric machines are considered[15].

A key issue related to the cylindrical stage is temperature elevation. Due to high energy density and the vacuum inner space of the stage, the heat generated at the magnetic core cannot be dissipated efficiently to the surroundings. The resulting high core temperature decreases the energy efficiency and potentially results in failure of the system. The only heat transfer mode allowed for the magnetic levitation stage is the conduction heat transfer through the stator base [4] since the convection heat transfer path is block by the vacuum environment, and the radiation heat transfer is negligible at typical system temperatures. In order to solve this thermal problem, we propose a cooling scheme wherein a water-flowing tube is inserted in the module base, so that the generated heat can easily escape via internal convection heat transfer to the outside.

For this purpose, the thermal performance of the proposed cooling scheme needs to be demonstrated and characterized. In this study, the heat dissipation from a cylindrical magnetic levitation stage is investigated numerically and experimentally. The stator is incorporated with the cooling pipe, and was analyzed by using finite element numerical simulation to investigate the effect of the electrical current, and the flow velocity of the cooling water.

Structure of the magnetic levitation stage design

A schematic diagram cylindrical electro-magnetic motor considered in this study is shown in Fig. 1. The whole assembly is used in a vacuum environment. This figure shows the front view of the coil module set. The module consists of a permanent magnet (rotor), six coil modules, each with a module base surrounding the rotor. A cooling tube is inserted in the module base to circulate the cooling water. During the actuating procedure, heat generated in the coil module cannot be dissipated through the inner space of the actuator, whereas the main thermal path is radial thermal conduction through the module base. Another thermal dissipation mechanism is a radiation from the surrounding vacuum chamber to an adjacent environment. Therefore, the coil module is the major concern in terms of thermal issues. A two dimensional (2-D) diagram for a coil module is shown in Fig. 1. The coil module consists of a module base with a cooling pipe, a spacer, and the coil. From figure1, cooling water flows to the left and comes out the right side. The coil modules are attached to the module base through the epoxy bonding as like Fig. 2. The epoxy part has a crucial role in dissipating the heat generated in the coil assembly to the cooling water. The thermally conductive epoxy (T7110, Epoxy technology Co. Ltd., MA, USA) was applied to enhance the heat conduction. The materials and dimensions of the components are summarized in Table 1. Each coil shown in Fig. 3 represents hundreds of copper windings. The coils are separated by spacers. The coils have an insulation coating to electrically disconnect the copper coil and aluminum spacer. Thermal epoxy is applied between the coil module and the module base for good mechanical and thermal connection. The size of the coil is 102.6 mm long × 42 mm high, 12.6 mm wide, and 7.7 mm thick. The coil base has dimensions of 102 mm × 86.4 mm with a thickness of 26.5 mm. The distance between the centers of the two pipe holes is 35 mm. The radius of curvature of the saddle is 94 mm. The diameter of the cooling pipe hole is 5 mm. The thickness of the epoxy layer is minimum 1.15 mm and maximum 3.1mm.

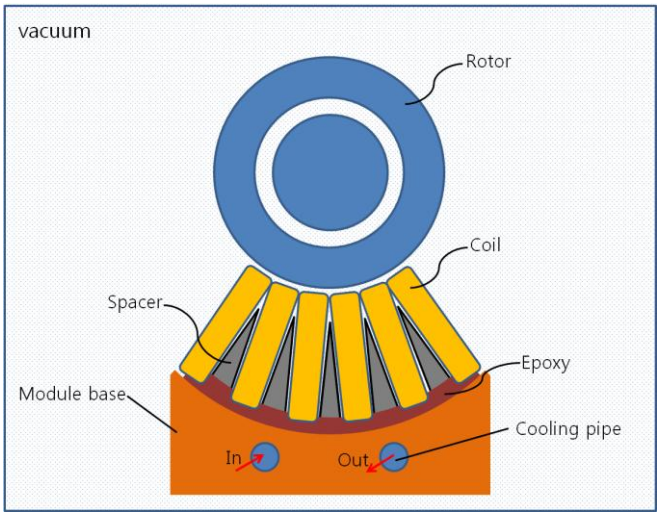

Fig. 1. Schematic diagram of an electro-magnetic motor.

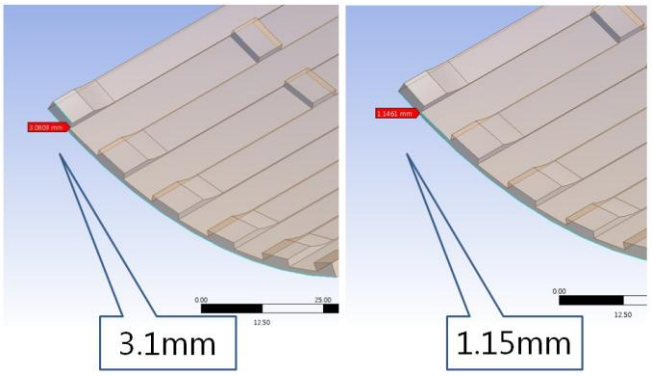

Fig. 2. Epoxy thickness.

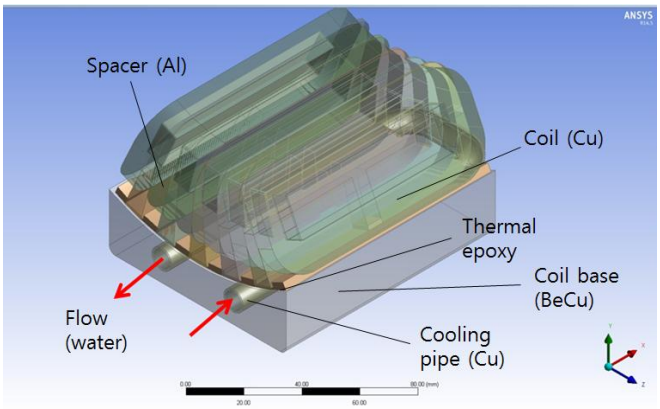

Fig. 3. Computational domain for numerical study.

Numerical Study

The computational domain considered in this study is shown in Fig. 3. The domain consists of a copper coil, an aluminum spacer between coils, a coil base made of beryllium copper, a copper cooling pipe, thermal epoxy between the coil module and the coil base, and water flowing inside the cooling pipe. We conducted a multi-physics simulation using the ANSYS commercial finite element software program (Workbench14, Ansys Inc., PA, USA). The program, which can simulate a thermal-electrical coupled problem, was used to analyze the temperature distribution in the system, as shown in Fig. 3.Since the problem involves convection heat transfer between the cooling water and the cooling pipe, the temperature solution for the multi-physical problem cannot be obtained with one computation. In order to solve this problem, we first solved the Joule heating rate generated in the coil without consideration of the flowing water. The coupling between heating and electrical fields is accounted for by simultaneously solving the following governing equations:

$$\nabla \cdot \lambda \nabla V = 0 \quad (1)$$

$$\rho c_p \frac{\partial T}{\partial t} - \nabla \cdot (k \nabla T) = \lambda |\nabla V|^2 \quad (2)$$

where V is electrostatic potential, λ is electrical conductivity, k is the thermal conductivity, T is temperature, ρ is density, c_p is specific heat, and t is time. Equation (1) corresponds to the electrical conduction equation, and Eq. (2) is the thermal conduction equation. The right hand side of Eq. (2)

corresponds to Joule heating induced by the electric current caused by the electrostatic potential gradient. The current density, *J*, has the following correlation with *V*:

$$\vec{J} = -\lambda \nabla V \quad (3)$$

Combining Eqs. (1), (2), and (3) yields the Joule heating distribution in the coil. Figure 4 shows the estimated current flux (this also indicates the heat flux) distribution in coil.

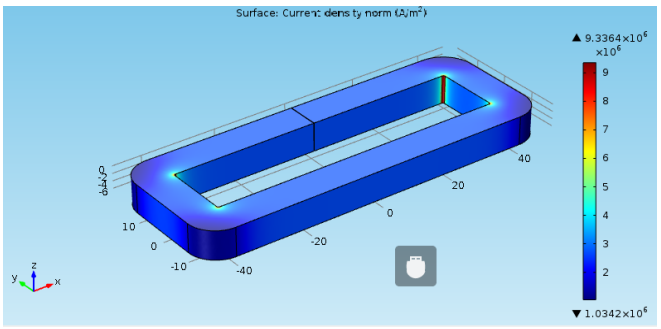

Fig. 4. Estimated current flux in the coil.

The estimated Joule heating distribution is then imported into the FEM package to solve the convection heat transfer problem and obtain the temperature distribution in the core. The governing equations are as follows:

$$\rho c_p \frac{\partial T}{\partial t} - \nabla \cdot (k \nabla T) = Q \quad (4)$$

Equation (4) represents the solid. *Q* denotes the heat generation per unit volume, and this is given as estimated in the previous stage. Equations (5) and (6) are for the fluid. Equation (5) is the Navier-Stokes equation, and Eq. (6) represents the energy equation. Thus,

$$\rho\left(\frac{\partial \vec{v}}{\partial t} + \vec{v} \cdot \nabla \vec{v}\right) = -\nabla P + \nabla^2 \vec{v} \quad (5)$$

$$\rho c_p \frac{\partial T}{\partial t} + \rho c_p \vec{u} \cdot \nabla T = \nabla \cdot \; k \nabla T \quad (6)$$

where $\vec{u}$ is the flow velocity vector. Natural convective boundary conditions were applied at the bottom surface of the coil base. Due to the vacuum environment, the other surfaces were defined as insulation boundary conditions. The thermophysical properties of the coil, coil base, spacer, thermal epoxy, and water were accurately estimated based on reports from the literature [8], as summarized in Table 1. The geometries of the computational domain were the same as those used in the experimental cases.

Table 1 Properties of materials used in the numerical study

	ρ (kg/m^3)	c_p(J/kgK)	k (W/mK)
Cu (coil, pipe)	8,933	195	387.6
Al (Spacer)	2,700	869	167
Epoxy T7110	1,500	1120	1
Water (20 ^{o}C)	1,000	4,180	0.6
BeCu (base)	8,250	1250	260

Results

The effect of the flow velocity on the temperature distribution in the coil module is illustrated in Fig. 5. In this figure, the first row corresponds to the plane-cut distribution with respect to the z axis, the second row is a perspective view, and the third row represents the quantitative values. The first column represents 0.1 m/s, 0.01 m/s, and no water case, respectively. As shown in the figure, the flow rate has a significant effect on the coil temperature. When 0.01 m/s water is applied, the coil temperature decreases by 55% compared with the no-water case. However, when the flow velocity is 0.1 m/s, the coil temperature decreases by only 17% compared with the 0.01 m/s case. This indicates that the entire thermal resistance of the coil module is dominated by high conduction thermal resistance. Therefore, applying cooling water has a significant effect on the temperature of the magnetic levitation stage, regardless of the flow rate of the cooling water. The convection heat transfer of the cooling water can be quantified as follows:

$$Q_{conv} = \dot{m} c_p \; T_{out} - T_{in} \quad (7)$$

where $\dot{m}$ is mass flow rate (kg/s), c_p is the specific heat of water, T_{out} is the outlet temperature of the water, and T_{in} is the inlet temperature of the water. This suggests that the convective heat transfer is approximately invariant when the flow rate is decoupled. Therefore, the contribution of conduction heat transfer is negligible with respect to the overall heat transfer.

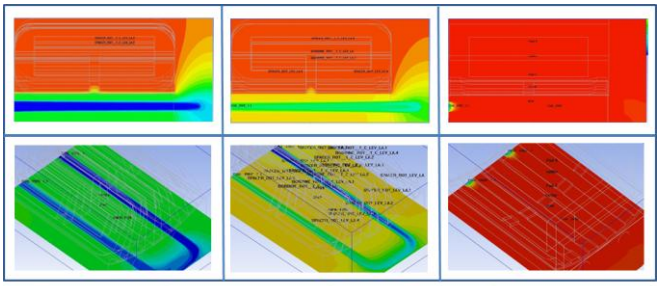

Flow velocity	Coil temp.	Water (in) temp.	Water (out) temp.
0.1 m/s	23.5°C	20°C	20.4°C
0.01m/s	28.45°C	20°C	24°C
No Water	63°C	20°C	63°C

Fig. 5. Temperature distribution vs. flow rate.

Figure 6 shows the estimated thermal expansion distribution of the coil module. The figure shows that the thermal stress is concentrated at the upper edge of the coil module. When no water is applied, the maximum thermal expansion is estimated to be 0.1 mm. When 0.1 m/s water is applied, the maximum thermal expansion decreases to 0.004 mm. Therefore, the cooling water has a significant effect on the mechanical stability of the magnetic levitation stage, as well as the thermal stability.

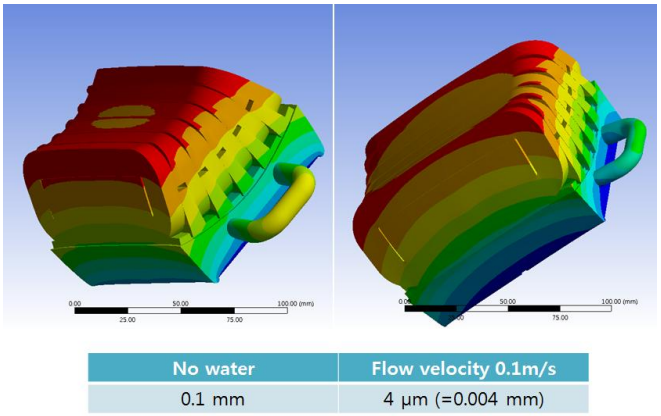

Fig. 6. Thermal expansion distribution in coil module.

Figure 7 shows the effect of the current and current phase on the maximum temperature of the coil (upper column) and outlet temperature of the water (lower column). In this numerical case, the inlet temperature of the cooling water and flow velocity were set to 10 °C and 0.0133 m/s, respectively. As shown in the figure, the current phase has a negligible effect on the temperature distribution. When the current is doubled, the maximum temperature of the coil significantly increases.

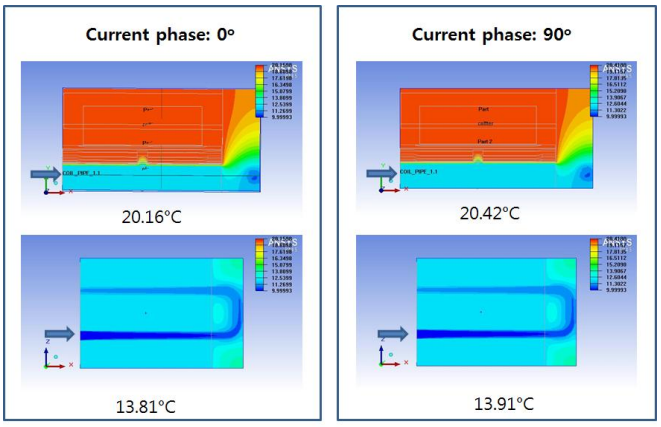

(a) I = 1 A.

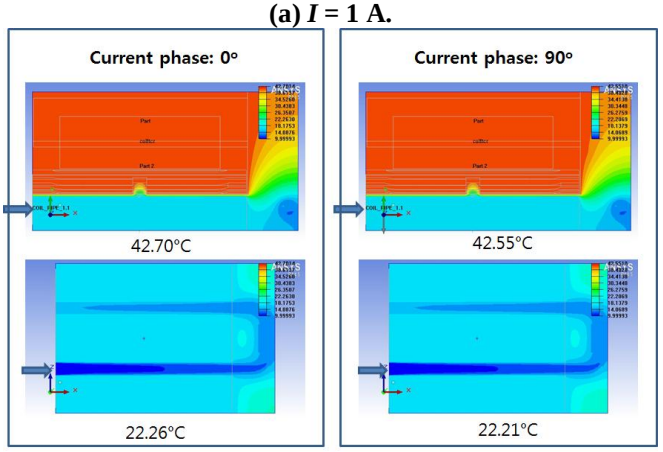

(b) I = 2 A.

Fig. 7. Effect of current and current phase on the temperature distribution of coil module.

The convective heat transfer rate was estimated by using Eq. (7). The heat dissipation of the 2 A system is four times larger than that of the 1 A system. This can be understood in terms of the Joule heating law:

$$Q = I^2 R \quad (8)$$

Therefore, the heat transfer from the magnetic levitation stage is numerically shown to obey the basic laws characterized by Eqs. (7) and (8).

Figure 8 shows a streamlined heat flow aournd the various components. Figure 8 indicate that the heat generated in the coils is dissipated out through the cooling water of the cooling pipe. Furthermore, the nearly half of the heat is transmitted to the inlet cooling pipe and the remaining heat is also transmitted to the outlet cooling pipe.

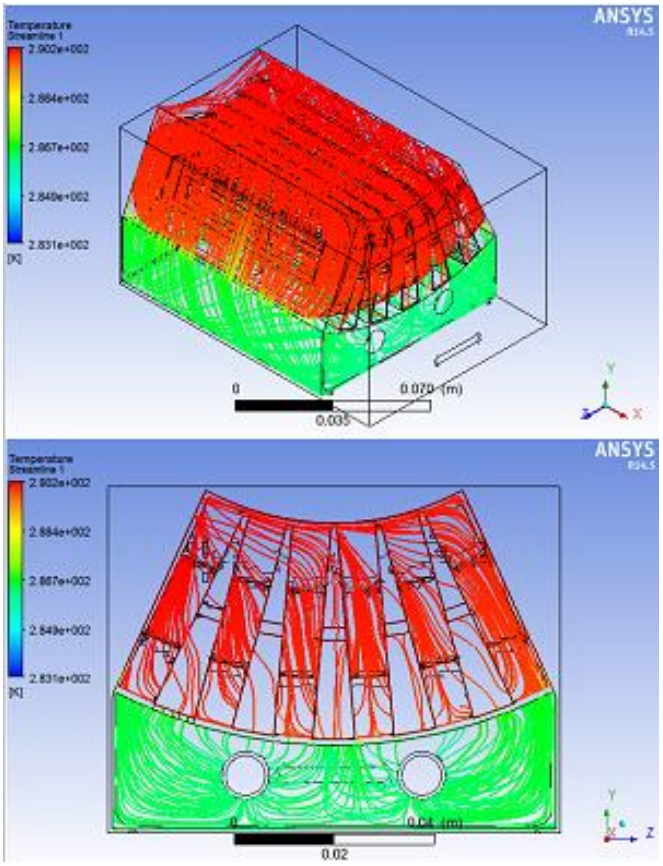

Fig. 8. Heat flow around the coil, module base and cooling pipe.

Conclusions

The heat dissipation from a cylindrical magnetic levitation stage was investigated numerically. A stator incorporated with a cooling pipe was analyzed using FEM numerical simulation in order to investigate the effect of the electrical current and the flow velocity of the cooling water. The results indicate that augmentation of the cooling pipe resulted in a significant enhancement in the heat dissipation performance of the magnetic levitation stage. The coil temperature is shown to decrease as the flow rate increases, or as the current decreases. The current phase is shown to have a negligible effect on the heat transfer from the stage. The suggested cooling scheme

sheds light on an optimal design for a vacuum-based electromagnetic system, which in turn could be applied to next-generation semiconductor manufacturing.

Acknowledgements
This research was supported by Basic Science Research Program through the National Research Foundation of Korea (NRF) funded by the Ministry of Education (NRF-2013R1A1A4A01009657).

References

[1] Van Engelen, G., Bouwer, A. G., "Two-step positioning device using Lorentz forces and a static gas bearing," U. S. Patents 5120034, June, 1992.

[2] Kim, J., Trumper, D. L., Lang, J. H., "Modeling and vector control of planar Magnetic Levitator," IEEE Trans. Industry Applications, Vol. 34, pp. 1254-1262, 1998.

[3] Sawyer, B. A., "Magnetic positioning device," U.S. Patent 3376578, April, 1968.

[4] Shan, X. S., Kuo, S. K., Zhang, J., and Menq, C. H., "Ultra precision motion control of a multiple degrees of freedom magnetic suspension stage," IEEE/ASME Trans. on Mechatronics, Vol. 7, No. 1, pp.67-78, 2002.

[5] Chen, M. Y., Wang, M. J., and Fu, L. C., "A Novel dual axis repulsive maglev guiding system with permanent magnet: modeling and controller design," IEEE/ASME Trans. on Mechatronics, Vol. 8, No.1, pp. 77-86, 2003.

[6] Jeon, J. W., Caraiani, M., Oh, H. S., and Kim, S., "Experiments of a novel magnetic levitation stage for wide area movements," J. Electrical Engineering Technology, Vol. 7, No. 4, pp. 558-563, 2012.

[7] Jeon, J. W., Lee, C. L., Oh, H. S., Kim, J. M., "Novel cylindrical magnetic levitation stage with high precision motion," 14th Int. Symposium on Magnetic Bearings, Linz, Austria, Auguest 11-14, 2014.

[8] Incropera, F. P., DeWitt, D. P., Fundamentals of Heat and Mass Transfer, Wiley, pp. 478-480, 2002.

[9] Q Chen, Xin-Gang Liang, Zeng-Yuan Guo " Entransy theory for the optimization of heat transfer – A review and update" International Journal of Heat and Mass Transfer 63 (2013) 65–81

[10] Huang Xuzhen, Liu Jiaxi, Zhang Chengming, and Li Liyi, "Calculation and Experimental Study on Temperature Rise of a High OverLoad Tubular Permanent Magnet Linear Motor", IEEE TRANS. ON PLASMA SCIENCE, VOL. 41, NO. 5, MAY 2013

[11] Xinmin Zhang, Qinfen Lu, Yuqiu Zhang, Xiaoyan Huang, Yunyue Ye, "Thermal Characteristics Study of a Water-cooled Permanent Magnet Linear Motor", *Proc. 2014 Ninth International Conference on Ecological Vehicles and Renewable Energies* (IEEE) 2014, 1-9.

[12] Jang, C.S., Kim, J.Y., Kim, Y.J., Kim, J.O., "Heat Transfer Analysis and Simplified Thermal Resistance Modeling of Linear Motor Driven Stages for SMT Applications", IEEE Trans. on Components and Technologies, Vol. 26, No. 3, pp.532-540, September, 2003.

[13] XuZhen Huang, Zhuoran Zhang, ChengMing Zhang, Bo Zhou, LiYi Li "Temperature Calculation for Tubular Linear Motor by the Combination of Thermal Circuit and Temperature Field Method Considering the Linear Motion of Air Gap.", IEEE Trans. Ind. Electron., vol. 61, no. 8, pp. 3923-3931, 2014

[14] T. A. Jankowski, F. C. Prenger, D. D. Hill, S. R. O'Bryan, K. K. Sheth, E. B. Brookbank, D. F. A. Hunt and Y. A. Orrego, "Development and validation of a thermal model for electric induction motors" IEEE Trans. Ind. Electron., vol. 57, no. 12, pp. 4043-4054, 2010

[15] A. Boglietti , A. Cavagnino , D. Staton , M. Shanel , M. Mueller and C. Mejuto "Evolution and modern approaches for thermal analysis of electrical machines" IEEE Trans. Ind. Electron., vol. 56, no. 3, pp. 871-882, 2009